Biochemical and Biophysical Research Communications 459 (2015) 493–497

Contents lists available at ScienceDirect

Biochemical and Biophysical Research Communications

journal homepage: www.elsevier.com/locate/ybbrc

Internal dynamics of F-actin and myosin subfragment-1 studied by quasielastic neutron scattering

Tatsuhito Matsuo [a], Toshiaki Arata [b], Toshiro Oda [c], Kenji Nakajima [d], Seiko Ohira-Kawamura [d], Tatsuya Kikuchi [d], Satoru Fujiwara [a, *]

[a] Quantum Beam Science Center, Japan Atomic Energy Agency, Tokai, Ibaraki 319-1195, Japan
[b] Department of Biological Sciences, Graduate School of Science, Osaka University, Toyonaka, Osaka 560-0043, Japan
[c] Graduate School of Science, University of Hyogo, Kamigori-cho, Ako-gun, Hyogo 678-1297, Japan
[d] Neutron Science Section, J-PARC Center, Tokai, Ibaraki 319-1195, Japan

ARTICLE INFO

Article history:
Received 10 February 2015
Available online 5 March 2015

Keywords:
Actin
Myosin
Protein dynamics
Quasielastic neutron scattering

ABSTRACT

Various biological functions related to cell motility are driven by the interaction between the partner proteins, actin and myosin. To obtain insights into how this interaction occurs, the internal dynamics of F-actin and myosin subfragment-1 (S1) were characterized by the quasielastic neutron scattering measurements on the solution samples of F-actin and S1. Contributions of the internal motions of the proteins to the scattering spectra were separated from those of the global macromolecular diffusion. Analysis of the spectra arising from the internal dynamics showed that the correlation times of the atomic motions were about two times shorter for F-actin than for S1, suggesting that F-actin fluctuates more rapidly than S1. It was also shown that the fraction of the immobile atoms is larger for S1 than for F-actin. These results suggest that F-actin actively facilitates the binding of myosin by utilizing the more frequent conformational fluctuations than those of S1.

1. Introduction

Many biological functions related to cell motility including muscle contraction are driven by the interaction between the partner proteins, actin and myosin. Myosin binds to the polymerized actin (F-actin), producing force by utilizing the hydrolysis energy of adenosine triphosphate. Structural aspect of this actin-myosin interaction has been extensively studied [1], and the recent structures of F-actin alone or decorated with myosin subfragment-1 (S1; the head region of the myosin molecule containing both the catalytic domain and the actin-binding sites) solved at the atomic level [2–4] have advanced significantly our understanding of the mechanism of this interaction in terms of the protein structures. F-actin is, however, a flexible molecule: F-actin changes its intrinsic flexibility upon nucleotide binding [5] and myosin binding [6], and F-actin has been proposed to adopt multiple structural conformations (structural polymorphism) [7]. S1 has also been found to exhibit structural flexibility: There is a wide range of variations in the orientation of the lever arm of the S1 molecule in the nucleotide-free state [8,9]. Furthermore, it has recently been shown that the compaction-expansion structural fluctuations of some loops at the actin-interface of S1 are essential for the proper functioning [10]. These findings suggest that the dynamical properties of both F-actin and S1 molecules are one of the key factors for the actin-myosin interaction. Thus, for full understanding of the mechanism of the actin-myosin interaction, exploration of the dynamical aspect of this interaction is required. In particular, investigation of possible differences in the dynamics between them is important because the degree of protein flexibility generally affects the conformational space that the protein can explore, and hence the rate of binding [11]. However, to the best of our knowledge, this point has not been addressed so far.

In this study, we compared the dynamics of F-actin and S1 by incoherent quasielastic neutron scattering (QENS). The motions of hydrogen atoms in protein molecules at pico-to nanosecond timescales can be probed by QENS. Since the incoherent neutron scattering cross-section of hydrogen atoms is more than 40 times larger than any other atoms found in protein samples, the measured QENS spectra arise predominantly from all the hydrogen

* Corresponding author. Quantum Beam Science Center, Japan Atomic Energy Agency, 2-4 Shirakata-Shirane, Tokai-mura, Naka-gun, Ibaraki 319-1195, Japan. Fax: +81 29 282 5822.
E-mail address: fujiwara.satoru@jaea.go.jp (S. Fujiwara).

http://dx.doi.org/10.1016/j.bbrc.2015.02.134
0006-291X/

atoms contained in the samples [12]. The measurements on the protein samples in D_2O-solvent thus provide the QENS spectra arising from the hydrogen atoms in the protein. Since the hydrogen atoms distribute homogeneously throughout the protein molecule, the information on the averaged dynamics over the whole protein is obtained by the QENS measurements. The motions at pico-to nanosecond timescales are essential for proper functions of proteins because the motions at these timescales act as a lubricant for the conformational changes of proteins at much slower timescales [13]. QENS thus provides quite a useful tool to investigate how the dynamics at these timescales is related to the functions of the proteins. Here, we carried out the QENS measurements on the D_2O solution samples of F-actin and S1, and detected the differences in dynamics between F-actin and S1.

2. Materials and methods

2.1. Sample preparation

Actin was purified from acetone powder of chicken breast muscle according to the procedure described [14]. The F-actin solution was prepared by polymerization of G-actin (monomeric form of actin) by adding $MgCl_2$ to the final concentration of 1 mM to the D_2O buffer containing 5 mM Tris-DCl (pD 8.0), 0.2 mM ATP, 0.1 mM $CaCl_2$, 1 mM NaN_3, and 0.5 mM dithiothreitol. The F-actin solution was then ultracentrifuged at 100,000 × g for 2 h. The obtained pellet was used as the sample for the neutron scattering experiments. The concentration of F-actin in the pellet was 150 mg/ml, which was determined spectrophotometrically by using the extinction coefficients $E^{1\%}_{280}$ of 11.1.

Myosin S1 was prepared by chymotryptic digestion of myosin from rabbit skeletal muscle as described [15], followed by dialysis against the D_2O buffer containing 20 mM Tris-DCl (pD 8.0), 150 mM KCl, 1 mM NaN_3, and 0.5 mM dithiothreitol. The S1 solution sample was concentrated to 80 mg/ml by using Amicon Ultra-15 centrifugal concentrators (MWCO: 30,000). The concentration of S1 was determined spectrophotometrically by using $E^{1\%}_{280}$ of 7.5.

Each solution sample was put in an aluminum flat cell of 0.4 mm thickness and sealed with indium wire for the neutron scattering experiments.

2.2. Neutron scattering experiments

The QENS measurements were carried out at 300 K using the cold-neutron disk-chopper spectrometer AMATERAS in MLF/J-PARC (Ibaraki, Japan) [16]. The measurements were done at multiple incident energy (multi-Ei measurements) with energy resolutions of 90.5, 26.6, and 11.5 μeV, at which the motions faster than 7, 25, and 57 ps are accessible, respectively. The energy resolution thus serves as a motion filter (an instrumental time window). A vanadium sample was measured for intensity correction and for defining the instrument energy resolutions. Subtraction of the spectra of the buffer from those of the sample with the appropriate scaling factor yielded the spectra arising from the proteins. The scaling factor was estimated from the weight of the proteins in the samples and the value of the partial specific volume of 0.73 cm^3/g. Note that, at 11.5 μeV energy resolution, the low statistics of the data hampered the detailed analysis of the QENS spectra in addition to the smaller range of the measurable momentum transfer Q (= $4\pi\sin\theta/\lambda$, where 2θ denotes the scattering angle and λ denotes the incident wavelength) than those at other energy resolutions. Analyses of the QENS spectra at 90.5 and 26.6 μeV energy resolutions are thus described here. Fitting of the measured spectra was done in the range of $-1.5\ \text{meV} \le \Delta E \le 1.5\ \text{meV}$ using IGOR Pro software (WaveMetrics, Lake Oswego, OR, USA).

3. Results and discussion

The measured QENS spectra can be described by the following equation [12]:

$$S(Q,\omega) = DW(Q) \times \exp(-\hbar\omega/2k_BT) \times \left[S_{global}(Q,\omega) \otimes S_{local}(Q,\omega) \otimes R(Q,\omega)\right] + B(Q) \quad (1)$$

where $\hbar\omega$ is the energy transfer, DW(Q) is the Debye-Waller factor, which accounts for vibrational modes, $\exp(-\hbar\omega/2k_BT)$ is the detailed balance factor, $S_{global}(Q, \omega)$ and $S_{local}(Q, \omega)$ denote the scattering function of the macromolecular global diffusion and the scattering function of the local atomic motions, respectively, R(Q, ω) is the resolution function of the spectrometer, and B(Q) is the background.

$S_{global}(Q, \omega)$ can be described by a Lorentzian function as

$$S_{global}(Q,\omega) = (1/\pi) \times \left(\Gamma_{global}(Q) \Big/ \left(\Gamma_{global}(Q)^2 + \omega^2\right)\right), \quad (2)$$

where Γ_{global} (Q) is the half-width at half-maximum (HWHM) of the Lorentzian function. $S_{local}(Q, \omega)$ can be described by

$$S_{local}(Q,\omega) = A_0(Q)\delta(\omega) + \sum_{i=1} A_i(Q) L_i(\Gamma_i, \omega) \quad (3)$$

where $A_0(Q)\delta(\omega)$ is the elastic component with $A_0(Q)$ being the fractional intensity and δ(ω) being the Dirac delta-function, and $A_i(Q)$ is the fractional intensity of the i-th Lorentzian function $L_i(\Gamma_i, \omega) = (1/\pi) \times (\Gamma_i\ (Q)/(\Gamma_i\ (Q)^2 + \omega^2))$, where $A_i(Q)$ meets the condition,

$$\sum_{i=0} A_i(Q) = 1. \quad (4)$$

The measured spectra of S1 and F-actin were shown in Fig. 1(A) and (B), respectively, together with the corresponding fits using Eq. (1), in which $S_{local}(Q, \omega)$ contains one Lorentzian function with its HWHM being Γ_{local} ($S_{local}(Q, \omega)$ is defined in Eq. (3)). Addition of the second Lorentzian did not improve the fit, judged from the values of the reduced-χ^2 (data not shown). The equation containing one Lorentzian was thus sufficient to fit to the measured spectra of both S1 and F-actin.

The Q^2-dependence of Γ_{global} of S1 is shown in Fig. 2(A). Γ_{global} increases linearly with increasing Q^2, indicating that the observed motions are free diffusion. The slope of the linear increase provides the translational diffusion coefficient, D_T. Although the values of Γ_{global} (Q) are smaller than those of the resolution function at low-Q region, about 10% broadening of the resolution width can be detected [17,18]. The estimated D_T values of S1 were $7.4 \pm 0.6 \times 10^{-7}$ cm^2/s at 90.5 μeV, and $7.4 \pm 0.2 \times 10^{-7}$ cm^2/s at 26.6 μeV. These are in the same order as those obtained for other protein solutions [17,19]. On the other hand, as shown in Fig. 2(B), the Q^2-dependence of Γ_{global} of F-actin showed different behavior from that of S1: The values of Γ_{global} at 90.5 μeV showed a plateau below $Q^2 \sim 1.2$ $Å^{-2}$, and then increased with increasing Q^2. This behavior is indicative of diffusive motions within a confined space rather than free diffusion [12]. The values of Γ_{global} at 26.6 μeV also showed similar behavior to that observed at 90.5 μeV though the features of the behavior were less significant. From the linear fits to the Q^2-region above 1.0 $Å^{-2}$ for 90.5 μeV and 0.4 $Å^{-2}$ for 26.6 μeV, respectively, the D_T values were estimated to be $6.6 \pm 0.3 \times 10^{-7}$ cm^2/s and $4.9 \pm 0.1 \times 10^{-7}$ cm^2/s, at 90.5 μeV and 26.6 μeV, respectively. Since the D_T value of the whole F-actin was estimated to be $2.4–7.7 \times 10^{-10}$ cm^2/s even at much lower

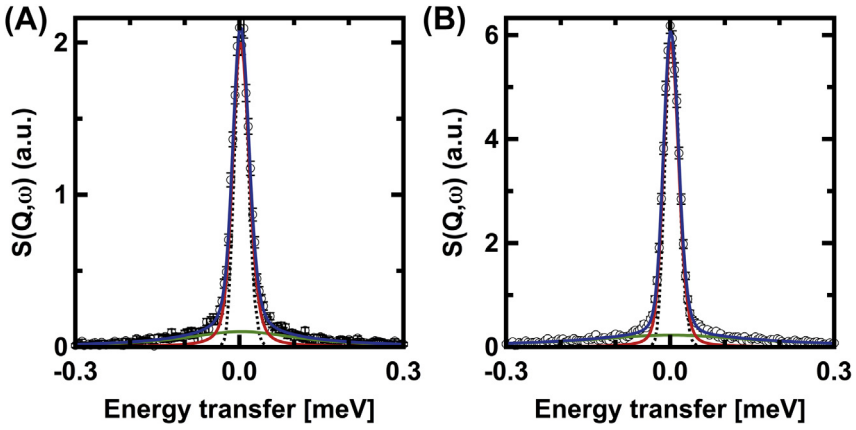

Fig. 1. Examples of the quasielastic neutron scattering spectra of (A) myosin S1 and (B) F-actin. The spectra at Q = 1.1 Å^{-1} at 26.6 μeV energy resolution are shown. Open circles in black denote the data points, and solid lines in blue, red, and green, denote the total fits, the elastic components, and the Lorentzian functions, respectively. Dotted lines denote the resolution functions. (For interpretation of the references to color in this figure legend, the reader is referred to the web version of this article.)

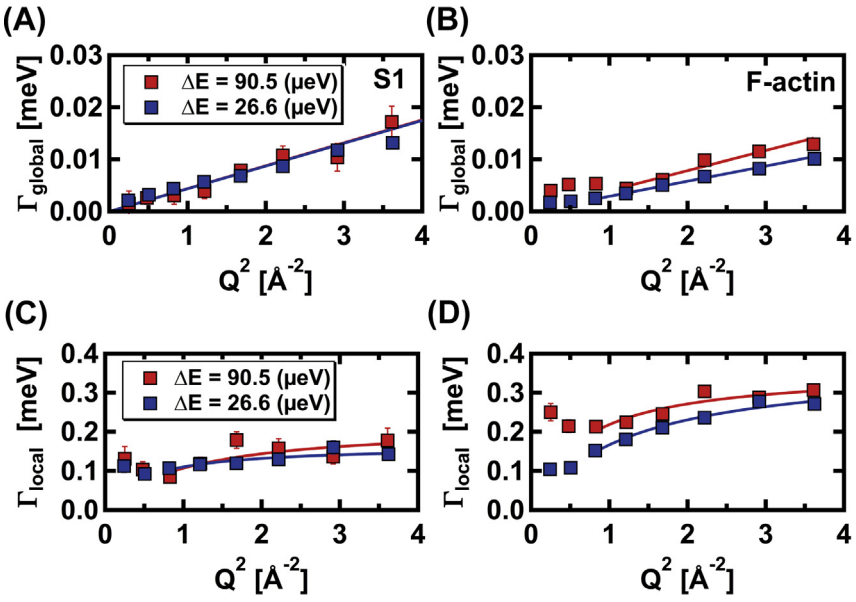

Fig. 2. Variations of the half width at half maximum of the Lorentzian functions as a function of Q^2. The Q^2-dependences of Γ_{global} (Q) of (A) S1 and (B) F-actin are shown with the corresponding linear fits. The Q^2-dependences of Γ_{local} (Q) of S1 and F-actin are shown in (C) and (D), respectively. The solid lines denote the fits using Eq. (5) in the main text. The error bars are within the symbols if not shown. The data obtained at the energy resolutions of 90.5 μeV and 26.6 μeV are shown in red and blue, respectively. (For interpretation of the references to color in this figure legend, the reader is referred to the web version of this article.)

concentration of 4 mg/ml than that employed in the present study [20], the values obtained here cannot arise from the diffusion of the whole F-actin. The D_T values obtained here are likely to arise from the diffusive motions of the individual actin molecules within F-actin. The motions of the individual actin molecules are confined by the contacts with the neighboring actin molecules, which is consistent with the observation described above. The different D_T values at the different energy resolutions imply that there is a distribution of the diffusive motions of the actin molecules in F-actin. It has been found that F-actin shows not only the bending motion but also the local unraveling into the two long-pitch helical strands [21]. It is thus likely that the interactions between the actin molecules are not identical over the entire length of F-actin. These differences would produce the distribution of the global motions of the individual actin molecules in F-actin.

The Q^2-dependence of Γ_{local} of S1 is shown in Fig. 2(C). At both 90.5 μeV and 26.6 μeV, Γ_{local} has the non-zero intercept at Q = 0, indicating the diffusive motions within a confined space. Γ_{local} increases asymptotically to a plateau value with increasing Q. This behavior can be fit by the equation based on the jump-diffusion model [12]:

$$\Gamma_{local}(Q) = D_T Q^2 \Big/ \left(1 + D_T Q^2 \tau_T\right), \quad (5)$$

where D_T denotes the translational diffusion coefficient of the jump-diffusion, and τ_T denotes the residence time. The plateau value is related to the residence time by the relation (the plateau value = $1/\tau_T$). The estimated values of τ_T were 3.0 ± 0.6 ps for 90.5 μeV and 4.0 ± 0.5 ps for 26.6 μeV, respectively. These values are typical for the globular proteins, such as those reported for myoglobin and lysozyme in solution [17]. Fig. 2(D) shows the Q^2-dependence of Γ_{local} of F-actin. Similar behavior to that of S1 was observed. Estimation of the residence times according to Eq. (5) yielded the τ_T values of 1.85 ± 0.09 ps at 90.5 μeV, and

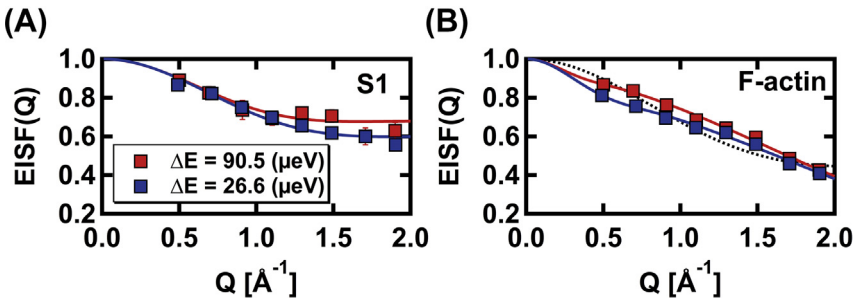

Fig. 3. The Q-dependence of the EISF. The EISF curves of (A) S1 and (B) F-actin as a function of Q are shown with the corresponding fits (solid lines). The color scheme is the same as in Fig. 2. The error bars are within the symbols if not shown. The dotted line in (B) denotes the representative fit to the data at 26.6 μeV using the equation containing one population of atoms undergoing diffusive motions within a confined space. (For interpretation of the references to color in this figure legend, the reader is referred to the web version of this article.)

1.8 ± 0.1 ps at 26.6 μeV, respectively. The τ_T values obtained for F-actin are about two times smaller than those obtained for S1 at both energy resolutions, indicating that the local motions of F-actin are faster than those of S1.

Geometry of the motions was characterized by analysis of the elastic incoherent structure factor (EISF), which is calculated as the ratio of the elastic intensity to the sum of the elastic and the quasielastic intensity. Fig. 3(A) shows the Q-dependence of the EISF of S1. Analysis of these EISF curves were done by fitting with the equation based on the model describing diffusive motions within a sphere:

$$\mathrm{EISF}(Q) = p_0 + p_1 \times (3j_1(Qa_1)/Qa_1)^2, \quad (6)$$

where p_0 denotes the fraction of the atoms observed as "immobile" within the instrumental time window, p_1 (= 1 − p_0) denotes the fraction of the atoms undergoing the diffusive motions in a confined sphere of the radius a_1, and j_1 denots the spherical Bessel function of the first kind of order 1 [22]. The best−fit parameters are summarized in Table 1. Fig. 3(B) shows the Q-dependence of EISF of F-actin. The EISF of F-actin is different from that of S1, indicating that the geometry of the local motions is different between them. The EISF of F-actin cannot be fit well with the equation containing only one population of the atoms undergoing the diffusive motions within a confined space as shown by dotted lines in Fig. 3(B). The EISF of F-actin was thus fit with the equation containing two diffusive motions within the spheres of the different radii:

$$\mathrm{EISF}(Q) = p_0 + p_1 \times (3j_1(Qa_1)/Qa_1)^2 + p_2 \times (3j_1(Qa_2)/Qa_2)^2, \quad (7)$$

where p_0 denotes the immobile fraction of atoms, p_1 and p_2 denote the fraction of atoms undergoing the diffusive motions within a sphere of the radii a_1 and a_2, respectively, and $p_0 + p_1 + p_2 = 1$. The obtained parameters are summarized in Table 1. As shown in Table 1, while a large fraction of the atoms in S1 is "immobile", a significant fraction of the atoms in F-actin was detected as mobile. This indicates that F-actin has a large population of the atoms moving faster than those of S1. These atoms in F-actin would allow it to search the conformational space more frequently than S1.

Table 1
Summary of the parameters on the geometry of the motions derived from the EISF analysis.

	p_0	p_1	a_1 [Å]	p_2	a_2 [Å]
Myosin S1					
90.5 μeV	0.68 (0.02)	0.32 (0.02)	2.7 (0.2)	–	–
26.6 μeV	0.60 (0.01)	0.40 (0.01)	2.4 (0.1)	–	–
F-actin					
90.5 μeV	0.1 (0.1)	0.08 (0.01)	8 (6)	0.8 (0.1)	1.1 (0.1)
26.6 μeV	0.0 (0.2)	0.18 (0.01)	5.8 (0.5)	0.8 (0.2)	1.0 (0.1)

Values in parenthesis are the standard deviations.

The major difference in the sample environment, which could have some effects on the protein dynamics, is the existence of 150 mM KCl in the S1 buffer. However, the effect of KCl, which is a well-known chaotrope, is to slightly increase the translational diffusion coefficient of water [23]. Moreover, it has been suggested that KCl increases protein flexibility [24]. It is therefore unlikely that the S1 dynamics is suppressed by the reduced mobility of water molecules, or by the direct binding of K^+ and/or Cl^- to the protein surface.

The direct comparison of the internal dynamics of F-actin and S1 here has demonstrated that the atoms in F-actin fluctuate more rapidly than those in S1, and that the fraction of the immobile atoms is smaller for F-actin than for S1. Since the QENS spectra arise as the sum of the spectra of all the individual hydrogen atoms distributed homogeneously in the proteins, the information obtained was on the average motions of (the hydrogen atoms within) the whole molecule. The differences observed here are therefore genuine differences in the average internal dynamics between F-actin and S1. These results thus indicate that, on average, the atoms in F-actin are more mobile than those in S1. This high mobility of the atoms in F-actin would allow it to search the conformational space frequently, which facilitates sampling of a variety of conformational substates. This is consistent with the notion of the structural polymorphism of F-actin [7], and the observation that F-actin switches between low- and high-FRET efficiency states, the latter of which is favored by the myosin-binding state [25]. Unlike myosin, the numerous actin-binding proteins have been found [26]. It has been shown that F-actin adopts slightly different conformations upon binding of the actin-binding proteins even belonging to the same superfamily [27,28]. It would be the enhanced flexibility of F-actin that enables the multiple interactions with the actin-binding proteins by adopting multiple conformations. The differences in the internal dynamics between F-actin and S1 detected here suggest that F-actin plays a more active role than myosin in the binding process, or in the initial phase of the actin-myosin interaction. Among the multiple conformations that F-actin can adopt, some of them would be more favorable for myosin to bind to F-actin. The results obtained here should serve as a basis for a new research direction, in which the dynamical aspect of the actin-myosin interaction is explored and thereby obtaining new insights into the mechanism of this interaction.

Conflict of interest

The authors declare no conflict of interest.

Acknowledgments

This work was supported by Grant-in-Aid for Scientific Research on Innovative Areas from the Ministry of Education, Culture, Sports, and Technology (Grant No. 23118720 to SF).

Transparency document

Transparency document related to this article can be found online at http://dx.doi.org/10.1016/j.bbrc.2015.02.134.

References

[1] M.A. Geeves, R. Fedorov, D.J. Manstein, Molecular mechanism of actomyosin-based motility, Cell. Mol. Life Sci. 62 (2005) 1462–1477.
[2] T. Fujii, A.H. Iwane, T. Yanagida, K. Namba, Direct visualization of secondary structures of F-actin by electron cryomicroscopy, Nature 467 (2010) 724–729.
[3] E. Behrmann, M. Müller, P.A. Penczek, H.G. Mannherz, D.J. Manstein, S. Raunser, Structrue of the rigor actin-tropomyosin-myosin complex, Cell 150 (2012) 327–338.
[4] B.H. Várkuti, Z. Yang, A. Malnasi-Czizmadia, Structural model of weak-binding actomyosin in the prepowerstroke state, J. Biol. Chem. 290 (2015) 1679–1688.
[5] H. Isambert, P. Venier, A.C. Maggs, A. Fattoum, R. Kassab, D. Pantaloni, M.F. Carlier, Flexibility of actin filaments derived from thermal fluctuations. Effect of bound nucleotide, phalloidin, and muscle regulatory proteins, J. Biol. Chem. 270 (1995) 11437–11444.
[6] T. Yanagida, F. Oosawa, Polarized fluorescence from epsilon-ADP incorporated into F-actin in a myosin-free single fiber: conformation of F-actin and changes induced in it by heavy meromyosin, J. Mol. Biol. 126 (1978) 507–524.
[7] V.E. Galkin, A. Orlova, G.F. Schroder, E.H. Egelman, Structural polymorphism in F-actin, Nat. Struct. Mol. Biol. 17 (2010) 1318–1323.
[8] N. Billington, D.J. Revill, S.A. Burgess, P.D. Chantler, P.J. Knight, Flexibility within the heads of muscle Myosin-2 molecules, J. Mol. Biol. 426 (2014) 894–907.
[9] S.A. Burgess, M.L. Walker, H.D. White, J. Trinick, Flexibility within myosin heads revealed by negative stain and single-particle analysis, J. Cell Biol. 139 (1997) 675–681.
[10] Q.-M. Nie, M. Sasai, T.P. Terada, Conformational flexibility of loops of myosin enhances the global bias in the actin-myosin interaction landscape, Phys. Chem. Chem. Phys. 16 (2014) 6441–6447.
[11] B.A. Shoemaker, J.J. Portman, P.G. Wolynes, Speeding molecular recognition by using the folding funnel: the fly-casting mechanism, Proc. Natl. Acad. Sci. 97 (2000) 8868–8873.
[12] M. Bée, Quasielastic Neutron Scattering, Adam Hilger, 1988.
[13] M.K.C.L. Brooks III, B.M. Pettitt, Proteins: A Theoretical Perspective of Dynamics, Structure and Thermodynamics, John Wiley & Sons, New York, 1990.
[14] T. Oda, K. Makino, I. Yamashita, K. Namba, Y. Maeda, Effect of the length and effective diameter of F-actin on the filament orientation in liquid crystalline sols measured by x-ray fiber diffraction, Biophys. J. 75 (1998) 2672–2681.
[15] A.G. Weeds, R.S. Taylor, Separation of subfragment-1 isoenzymes from rabbit skeletal muscle myosin, Nature 257 (1975) 54–56.
[16] K. Nakajima, S. Ohira-Kawamura, T. Kikuchi, M. Nakamura, R. Kajimoto, Y. Inamura, N. Takahashi, K. Aizawa, K. Suzuya, K. Shibata, T. Nakatani, K. Soyama, R. Maruyama, H. Tanaka, W. Kambara, T. Iwahashi, Y. Itoh, T. Osakabe, S. Wakimoto, K. Kakurai, F. Maekawa, M. Harada, K. Oikawa, R.E. Lechner, F. Mezei, M. Arai, AMATERAS: a cold-neutron disk chopper spectrometer, J. Phys. Soc. Jpn. 80 (2011). SB028.
[17] J. Perez, J.M. Zanotti, D. Durand, Evolution of the internal dynamics of two globular proteins from dry powder to solution, Biophys. J. 77 (1999) 454–469.
[18] S. Fujiwara, M. Plazanet, F. Matsumoto, T. Oda, Internal motions of actin characterized by quasielastic neutron scattering, Eur. Biophys. J. 40 (2011) 661–671.
[19] T. Matsuo, F. Natali, M. Plazanet, G. Zaccai, S. Fujiwara, Dynamics of cardiomyopathy-causing mutant of troponin measured by neutron scattering, J. Phys. Soc. Jpn. 82 (2013) SA0201–SA0205.
[20] J. Käs, H. Strey, J.X. Tang, D. Finger, R. Ezzell, E. Sackmann, P.A. Janmey, F-actin, a model polymer for semiflexible chains in dilute, semidilute, and liquid crystalline solutions, Biophys. J. 70 (1996) 609–625.
[21] A. Bremer, R.C. Millonig, R. Sütterlin, A. Engel, T.D. Pollard, U. Aebi, The structural basis for the intrinsic disorder of the actin filament: the lateral slipping model, J. Cell Biol. 115 (1991) 689–703.
[22] F. Volino, A.J. Dianoux, Neutron incoherent scattering law for diffusion in a potential of spherical symmetry: general formalism and application to diffusion inside a sphere, Mol. Phys. 41 (1980) 271–279.
[23] P. Ben Ishai, E. Mamontov, J.D. Nickels, A.P. Sokolov, Influence of ions on water diffusion–a neutron scattering study, J. Phys. Chem. B 117 (2013) 7724–7728.
[24] K. Toth, E. Sedlak, M. Sprinzl, G. Zoldak, Flexibility and enzyme activity of NADH oxidase from Thermus thermophilus in the presence of monovalent cations of Hofmeister series, Biochim. Biophys. Acta 1784 (2008) 789–795.
[25] J. Kozuka, H. Yokota, Y. Arai, Y. Ishii, T. Yanagida, Dynamic polymorphism of single actin molecules in the actin filament, Nat. Chem. Biol. 2 (2006) 83–86.
[26] S.J. Winder, K.R. Ayscough, Actin-binding proteins, J. Cell. Sci. 118 (2005) 651–654.
[27] C.A. Moores, N.H. Keep, J. Kendrick-Jones, Structure of the utrophin actin-binding domain bound to F-actin reveals binding by an induced fit mechanism, J. Mol. Biol. 297 (2000) 465–480.
[28] D. Hanein, N. Volkmann, S. Goldsmith, A.M. Michon, W. Lehman, R. Craig, D. DeRosier, S. Almo, P. Matsudaira, An atomic model of fimbrin binding to F-actin and its implications for filament crosslinking and regulation, Nat. Struct. Biol. 5 (1998) 787–792.